Cardiovascular Research (2011) **91**, 456–464
doi:10.1093/cvr/cvr103

# IQGAP1 regulates ERK1/2 and AKT signalling in the heart and sustains functional remodelling upon pressure overload

**Mauro Sbroggiò[1], Daniela Carnevale[2], Alessandro Bertero[1], Giuseppe Cifelli[2], Emanuele De Blasio[1], Giada Mascio[2], Emilio Hirsch[1], Wadie F. Bahou[3], Emilia Turco[1], Lorenzo Silengo[1], Mara Brancaccio[1], Giuseppe Lembo[2,4], and Guido Tarone[1]***

[1]Dipartimento di Genetica, Biologia e Biochimica, Molecular Biotechnology Center, Università di Torino, via Nizza, 52, 10126 Torino, Italy; [2]Dipartimento di Angiocardioneurologia, I.R.C.C.S. 'Neuromed', Pozzilli, IS, Italy; [3]Department of Medicine, Stony Brook University, Stony Brook, NY 11794, USA; and [4]Dipartimento di Medicina Molecolare, Università 'La Sapienza' di Roma, 00161 Roma, Italy

*Received 29 October 2010; revised 31 March 2011; accepted 6 April 2011; online publish-ahead-of-print 14 April 2011*

**Time for primary review: 25 days**

**Aims** The Raf-MEK1/2-ERK1/2 (ERK1/2—extracellular signal-regulated kinases 1/2) signalling cascade is crucial in triggering cardiac responses to different stress stimuli. Scaffold proteins are key elements in coordinating signalling molecules for their appropriate spatiotemporal activation. Here, we investigated the role of IQ motif-containing GTPase-activating protein 1 (IQGAP1), a scaffold for the ERK1/2 cascade, in heart function and remodelling in response to pressure overload.

**Methods and results** IQGAP1-null mice have unaltered basal heart function. When subjected to pressure overload, IQGAP1-null mice initially develop a compensatory hypertrophy indistinguishable from that of wild-type (WT) mice. However, upon a prolonged stimulus, the hypertrophic response develops towards a thinning of left ventricular walls, chamber dilation, and a decrease in contractility, in an accelerated fashion compared with WT mice. This unfavourable cardiac remodelling is characterized by blunted reactivation of the foetal gene programme, impaired cardiomyocyte hypertrophy, and increased cardiomyocyte apoptosis. Analysis of signalling pathways revealed two temporally distinct waves of both ERK1/2 and AKT phosphorylation peaking, respectively, at 10 min and 4 days after aortic banding in WT hearts. IQGAP1-null mice show strongly impaired phosphorylation of MEK1/2-ERK1/2 and AKT following 4 days of pressure overload, but normal activation of these kinases after 10 min. Pull-down experiments indicated that IQGAP1 is able to bind the three components of the ERK cascade, namely c-Raf, MEK1/2, and ERK1/2, as well as AKT in the heart.

**Conclusion** These data demonstrate, for the first time, a key role for the scaffold protein IQGAP1 in integrating hypertrophy and survival signals in the heart and regulating long-term left ventricle remodelling upon pressure overload.

**Keywords** IQGAP1 • MAPKs • AKT • Heart hypertrophy • Pressure overload

## 1. Introduction

Heart failure represents one of the leading causes of mortality and is often the final stage of several overload cardiomyopathies, such as aortic stenosis, hypertension, and myocardial infarction. These cardiovascular diseases impose a haemodynamic overload on left ventricular (LV) walls, triggering a multifaceted process of tissue remodelling. LV hypertrophy is the initial phase of this complex response, characterized by an increase in wall thickness, which facilitates counterbalancing of the increase in LV wall stress and maintenance of cardiac function. This process involves a temporally regulated pattern of activation of several intracellular signalling pathways controlling the coordinate interplay between responses of different cardiac tissue components, namely cardiomyocyte growth and survival, capillary formation, and stroma deposition. However, long-standing haemodynamic overload is followed by later stages of

* Corresponding author. Tel: +39 011 6706433; fax: +39 011 6706432, E-mail: guido.tarone@unito.it

maladaptive tissue remodelling, characterized by thinning of LV walls and decreased global cardiac function, that eventually promote the transition towards heart failure. The molecular mechanisms involved in this transition are poorly defined and are likely to be dependent on the alteration of signalling pathways leading to cardiomyocyte loss, inflammation, and fibrosis.

Critical signalling pathways in cardiac remodelling include the extracellular signal-regulated kinases 1/2 (ERK1/2) cascade along with protein kinase B (AKT),[1] which are involved in cardiac hypertrophic growth, as well as in protection from apoptosis in response to a variety of stimuli. The ERK1/2 kinases are the final elements of a cascade in which the G-protein RAS activates the mitogen-activated protein kinase kinase kinase (MAPKKK) Raf, leading to the activation of the MAPKK MEK1/2, which in turn activates the MAPK ERK1/2. Scaffold proteins are crucial regulators of this signalling cascade due to their ability to bind to multiple members of this signalling pathway tethering them into complexes. In doing so, scaffold molecules boost the signal flux and also mediate crosstalk with other pathways. More generally, scaffolds assemble signalling cascade components into complexes by preventing unnecessary interactions between signalling proteins, and enhance signalling efficiency by increasing the proximity of components in the scaffold complex. The best characterized Raf-MEK-ERK scaffold protein is KSR, equivalent of Ste5, the well-studied yeast MAPK scaffold protein.[2] KSR is a positive regulator of this pathway and binds to all three kinases in the cascade.[3] β-Arrestin has also been characterized as an ERK cascade scaffold protein in response to β -adrenergic stimulation in hearts.[4] Emerging evidence indicates that the widely expressed protein IQGAP1 (IQ motif-containing GTPase-activating protein 1) acts as a scaffold for the MAPK cascade by binding b-Raf, MEK1/2 and ERK1/2, and regulating their activation in response to epidermal growth factor (EGF) in fibroblasts and epithelial cells.[5]

IQGAPs comprise three multidomain proteins (IQGAP1, IQGAP2, and IQGAP3) sharing a similar domain structure and with considerable sequence homology. IQGAP proteins have a different pattern of expression in mammalian tissues, and IQGAP1 is the only one that has been detected in the myocardium.[6] IQGAP1 contains different domains: calponin homology domain (CHD), polyproline protein–protein domain (WW), IQ motif (IQ), Ras GTPase-activating protein-related domain (GRD) and RasGAP_C-terminus (RGCT). The CHD is responsible for IQGAP1 binding to actin filaments; the IQ motif associates with calcium/calmodulin, b-Raf, and MEK1/2; the WW domain is able to associate with ERK1/2, and the RGCT domain binds to β-catenin and E-cadherin. Notably, the GRD domain does not facilitate GTPase activity; rather, this domain directly interacts with and stabilizes activated Rac1 and Cdc42. Thanks to the interaction with different molecular partners, IQGAP1 regulates many cellular functions, including cell proliferation, differentiation, adhesion, and migration.[6]

Here, we show that IQGAP1 in the heart acts as a scaffold molecule for both c-Raf-MEK1/2-ERK1/2 and AKT and is required for a specific, temporally regulated wave of both ERK1/2 and AKT signalling in response to pressure overload. Moreover, under these stress conditions, IQGAP1-null hearts fail to properly reactivate the foetal gene programme and undergo increased cardiomyocyte apoptotic death. Interestingly, mice lacking IQGAP1 display normal heart function in basal conditions and develop a normal compensatory hypertrophic response in the early phase of pressure overload. However, upon prolonged pressure overload, mutant mice show an accelerated transition towards maladaptive remodelling characterized by LV walls thinning and impaired contractility and ejection fraction (EF%) compared with WT animals. These data highlight an important role for IQGAP1 in ERK1/2 and AKT signalling in the heart and implicate IQGAP1 as a candidate for regulating the switch from adaptive to maladaptive cardiac remodelling in response to prolonged haemodynamic overload.

# 2. Methods

## 2.1 Mice and surgical procedures

IQGAP1-null mice of the SV129 strain were generated as described.[7] Two-month-old male mice were used in all experiments. The use of animals was in compliance with the *Guide for the Care and Use of Laboratory Animals* published by the US National Institutes of Health and was approved by the Animal Care and Use Committee of Turin University.

Chronic pressure overload was imposed to the LV through transverse aortic banding (AB), as previously described.[8]

## 2.2 Echocardiographic analyses

Serial echocardiographic evaluations were assessed in mice in basal conditions and during chronic pressure overload (1, 3, 5, 9, and 12 weeks after banding) as described.[9] Echocardiographic analysis was performed in mice anaesthetized with tribromoethanol (175 mg/kg), using a Vevo 770 (Visualsonics, Inc., Canada) device equipped with a 30 MHz probe. An LV M-mode tracing was obtained using the 2D parasternal short-axis imaging as a guide. End-diastolic interventricular septum (IVSd), posterior wall thicknesses (LVPWd), and LV internal diameter (LVIDd) were measured. Relative wall thickness (RWT), EF%, and fractional shortening (FS%) were calculated according to standard formulas. All measurements were performed at a heart rate comparable in both wild-type (WT) and IQGAP1-null mice (beats per minute; WT, basal 512 $\pm$ 3, 1-week AB 511 $\pm$ 4, 3-week AB 507 $\pm$ 4, 5-week AB 513 $\pm$ 6, 9-week AB, 12-week AB 517 $\pm$ 3; IQGAP1-null, basal 518 $\pm$ 5, 1-week AB 514 $\pm$ 4, 3-week AB 508 $\pm$ 2, 5-week AB 512 $\pm$ 2, 9-week AB 511 $\pm$ 3, 12-week AB 514 $\pm$ 2). A systolic trans-stenotic gradient was measured by echo Doppler (Vevo 770, Visualsonics), positioning the probe on AB. All mice analysed showed a pressure gradient comparable in both WT and IQGAP1-null mice (WT, 1-week AB 84 $\pm$ 5, 3-week AB 89 $\pm$ 2, 5-week AB 90 $\pm$ 2, 9-week AB 89 $\pm$ 1, 12-week AB 89 $\pm$ 2; IQGAP1-null, 1-week AB 85 $\pm$ 3, 3-week AB 89 $\pm$ 4, 5-week AB 88 $\pm$ 3, 9-week AB 89 $\pm$ 2, 12-week AB 90 $\pm$ 3).

## 2.3 Cell cultures, immunoprecipitations, and western blots

Neonatal mouse cardiomyocytes were isolated from 1-day-old 129sv and IQGAP1-null mice. Fibroblasts were removed by two rounds of pre-plating for 2 h on plastic tissue culture dishes. Cardiomyocytes were plated on gelatin/fibronectin-coated dishes and maintained in DMEM-M199 medium, 10% horse serum (Gibco), and 5% FBS (Gibco).

Neonatal mouse cardiac fibroblasts collected by pre-plating were maintained in DMEM 10% FCS for 48 h, starved for 24 h in DMEM 1% FCS, and stimulated with 10 ng/mL TGFβ1 (Peprotech) for 36 h for RNA analysis and 48 h for immunofluorescence.

For immunoprecipitation experiments, hearts were homogenized in lysis buffer—50 mM HEPES, 100 mM NaCl, 0.1% Na-deoxycholate, 0.1% Triton X-100, 1 mM EGTA, 2 mM EDTA—containing Roche Complete protease inhibitor cocktail, 10 mM NaF, 1 mM PMSF, 1 mM $Na_3VO_4$. Protein extracts were clarified with three sequential centrifugations at 14 000 r.p.m. at 4°C. Immunoprecipitation experiments were performed for 2 h at 4°C using 5 mg of total heart protein extract, 5 μg of anti-AKT, and 20 μL of protein G sepharose (GE) (see Supplementary material online, Methods).

### 2.4 Recombinant proteins

Expression vectors encoding maltose-binding protein (MBP) fused to melusin were prepared as previously described.[10] To produce recombinant MBP-fused IQGAP1 fragments, nucleotide sequences encoding for the protein fragments were cloned in pMAL C2 vector. MBP fusion proteins were produced in *Escherichia coli* BL21 bacterial strain and then purified on Sepharose amylose (New England Biolabs) according to the manufacturer's instructions.

### 2.5 Pull-down assay

Frozen heart samples were homogenized with an Ultra-Turrax (VWR) in 1% Triton TBS with protease and phosphatase inhibitors, centrifuged three times at 14 000 r.p.m. at 4°C, and ~3 mg of total protein extract was used for the pull-down assay. MBP-fused IQGAP1 fragments were purified from bacterial protein extracts using an amylose resin (GE) for 1 h at 4°C. Resin was washed five times with 1% Triton TBS, and 5 μg of recombinant protein was incubated in agitation for 2 h with 3 mg of total heart protein extract. Resin was washed 10 times with 1% Triton TBS and resuspended in Laemmli buffer. Pulled-down samples were analysed by western blot.

### 2.6 RNA extraction and real-time PCR

Frozen heart samples were homogenized in 1 mL of TRIzol reagent (Invitrogen), and total RNA was purified following manufacturer's protocol. TaqMan real-time PCR was performed using Universal Probe Library System (Roche) and specific primers for each target (Supplementary Methods).

### 2.7 Histological analyses

Heart sections were stained with haematoxylin and eosin, picrosirius red, Alexa488-labelled lectin from Griffonia Simplicifolia and probed with In Situ Cell Death Detection Kit TMR red (Roche) and anti-CD18 (BMA Biomedicals) antibodies as described.[11] Cardiomyocyte cross-sectional areas and fibrosis were measured using MetaMorph Software.

### 2.8 Renin activity assay

Fifty microlitres of mouse plasma was assayed for renin activity, using fluorimetric SensoLyte 520 Renin Assay Kit (Anaspec) following the manufacturer's instructions. Fluorescence has been detected on a Glomax luminometer (Promega).

### 2.9 Statistical analysis

The data are presented as mean ± SE. Differences among groups were tested by two-way ANOVA followed by Bonferroni's post hoc test. All statistical analyses were performed using GraphPad Prism 4 (GraphPad Software version 4.0).

## 3. Results

### 3.1 IQGAP1-null mice showed impaired heart function after long-standing pressure overload

Since IQGAP1 expression has not been previously characterized at the cellular level in the myocardium, we isolated cardiac fibroblasts and cardiomyocytes from neonatal mouse hearts and analysed the presence of IQGAP1 by western blotting. As shown in *Figure 1A*, IQGAP1 is expressed in cardiomyocytes as well as in fibroblasts.

To investigate the impact of IQGAP1 on cardiac structure and function, we took advantage of IQGAP1-null mice which are healthy and viable.[7] As shown in *Figure 1B–G*, echocardiographic analysis showed that lack of IQGAP1 expression does not affect cardiac morphology or function in basal conditions. IQGAP1-null and WT mice were then exposed to pressure overload by surgical AB, and LV remodelling was monitored over time by echocardiographic analysis (*Figure 1B–G*). AB induced a similar pressure overload in IQGAP1-null and WT mice (systolic pressure gradient: 84 ± 5 mmHg for WT and 85 ± 3 mmHg for IQGAP1-null mice; NS). After 1 week of pressure overload, IVSd and LVPWd increased to a similar extent (*Figure 1B* and *C*) in both mice groups. Similarly, IQGAP1-null and WT mice reduced LVIDd (*Figure 1D*) and fully retained the systolic contractile function (FS and EF) (*Figure 1E* and *F*). Thus, after 1 week of AB, IQGAP1-null mice developed a concentric LV hypertrophic response, comparable with that observed in WT mice, as evidenced also by the similar increase in RWT in both groups (*Figure 1G*). Furthermore, 1 week after AB, the ratio of the blood flow Doppler peak (*E*) at mitral inflow to the tissue movement Doppler peak (*e′*) at the lateral mitral annulus (*E*/*e′*), indicating diastolic function, was only slightly increased in both IQGAP1-null and WT mice, as compared with sham (see Supplementary material online, *Table S1*).

Since the presence of the chronic stimulus can affect the heart response in the long term, we examined the functioning of the heart during additional 11 weeks of AB. Interestingly, after 3 weeks of AB, though pressure overload was still similar in both mouse strains (see Methods), the thickness of IVSd (*Figure 2A*) and LVPWd (*Figure 2B*) in IQGAP1-null mice started to regress and LVIDd increased (*Figure 2C*) while WT mice retained the hypertrophic cardiac remodelling. These differences between genotypes became significant at 5 weeks for LVIDd and IVSd, and at 12 weeks for LVPWd vs. 1 week. At 9 and 12 weeks of AB, also FS (*Figure 2D*), EF (*Figure 2E*), and RWT (*Figure 2F*) were significantly reduced in IQGAP1-null mice compared with WT.

These data indicate that IQGAP1 is dispensable for the development of ventricular hypertrophy and preservation of heart function in the early phase of pressure overload, but is required to sustain functional remodelling in the presence of long-standing haemodynamic overload.

### 3.2 IQGAP1-null mice show impaired cardiomyocyte hypertrophy and increased apoptosis upon pressure overload

The unfavourable remodelling of IQGAP1-null mice was better characterized by histological analysis. Hearts in basal conditions showed no difference in the amount of stromal tissue, capillary density, inflammatory cells, cardiomyocyte size, and apoptosis between the two genotypes (*Figures 3A–E* and Supplementary material online, *Figure S1A*), demonstrating that the absence of IQGAP1 does not affect cardiac tissue organization.

After 1 week of AB, cardiomyocyte apoptosis was significantly higher in IQGAP1-null mice compared with WT (*Figure 3E*). Consistent with this finding, the level of the anti-apoptotic protein Bcl-XL was lower and that of the pro-apoptotic protein Bad was higher in IQGAP1-null compared with WT (*Figure 3F* and *G*); notably, these differences were not present in sham-operated animals (*Figure 3H* and *I*). In addition, analysis of foetal gene expression (*Figure 3J–M*) indicated that whereas WT mice after 1 week of AB showed increased transcription of atrial natriuretic peptide (ANP) and β-myosin heavy chain (β-MHC), IQGAP1-null mice showed a greatly impaired response (*Figure 3J* and *L*).

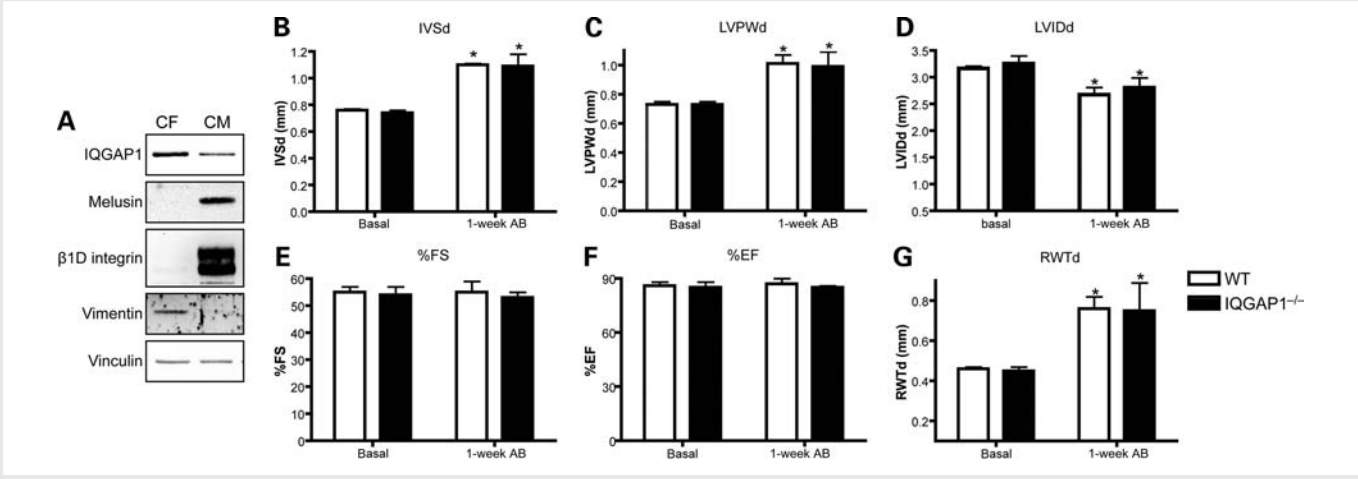


**Figure 1** IQGAP1-null mice develop a cardiac hypertrophy similar to WT mice after 1-week AB. (*A*) Western blot analysis on protein extracts from cardiac fibroblasts (CF) and cardiomyocytes (CM) from newborn WT mice. β1D integrin and vimentin were used as markers for cardiomyocytes and fibroblasts, respectively. Vinculin was used as a loading control. (*B*–*F*) Echocardiographic analysis of WT and IQGAP1-null mice (IQGAP1$^{-/-}$) in basal conditions and after 1 week of AB. IVSd, diastolic intraventricular septum thickness; LVPWd, diastolic left ventricle posterior wall thickness; LVIDd, diastolic left ventricle inner diameter; RWT, relative wall thickness in diastole; %FS, fractional shortening. *$P < 0.05$ vs. basal ($n = 10$ hearts/group).

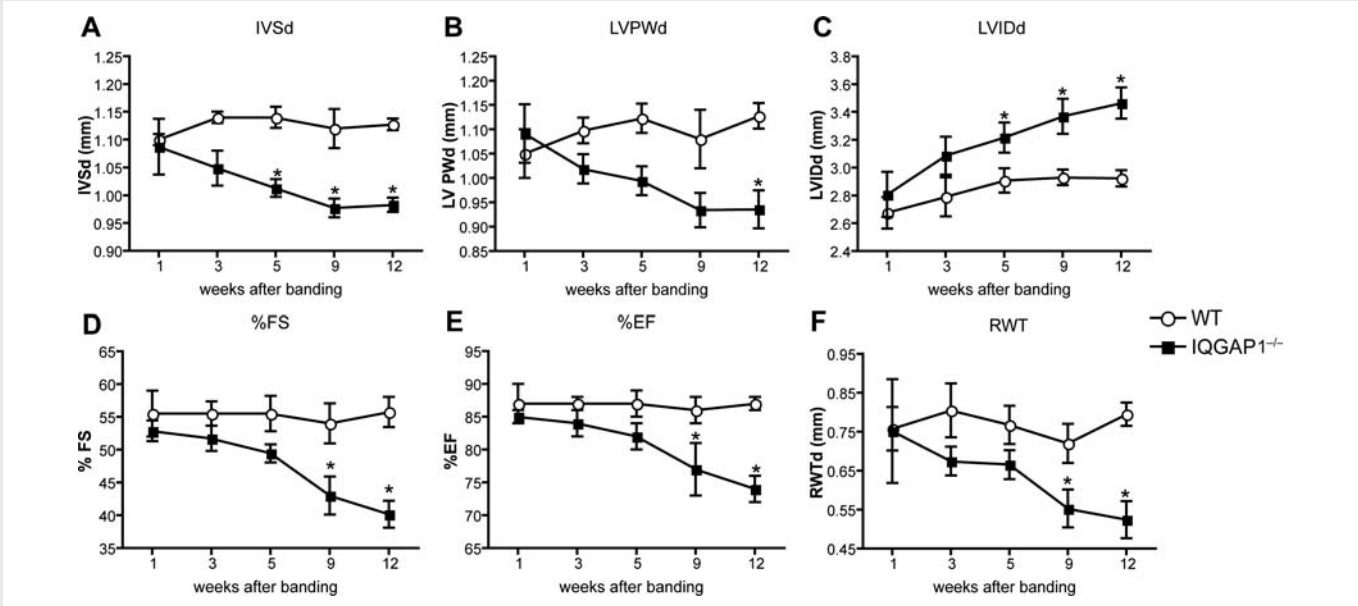


**Figure 2** IQGAP1-null mice showed impaired heart function after 12 weeks of AB. (*A*–*F*) Echocardiographic parameters acquired at the indicated time points (weeks of AB) from wild type (WT) and IQGAP1-null mice (IQGAP1$^{-/-}$) subjected to pressure overload. IVSd, diastolic intraventricular septum thickness; LVPWd, diastolic left ventricle posterior wall thickness; LVIDd, diastolic left ventricle inner diameter; RWT, relative wall thickness in diastole; %FS, fractional shortening. *$P < 0.05$ between groups ($n = 10$ hearts/group).

No major alterations, however, were observed in cardiomyocyte hypertrophy (*Figure 3D*), expression of extracellular matrix genes and pro-fibrotic cytokines (Supplementary material online, *Figure S2A–E*), matrix degrading enzymes (Supplementary material online, *Figure S2F*), HIF-1α, and VEGF between IQGAP1-null and WT mice after 1 week of AB (Supplementary material online, *Figure S2G* and *H*). In addition, activation of the renin–angiotensin system response to 1-week AB, as assessed by plasma renin activity, did not differ between IQGAP1-null and WT mice (Supplementary material online, *Figure S2I*).

Analysis of hearts subjected to 12 weeks of pressure overload indicated no difference in fibrosis (*Figure 3A* and Supplementary material online, *Figure S1A*), capillary density (*Figure 3B* and Supplementary material online, *Figure S1B*), and inflammatory cell infiltration (*Figure 3C*) between IQGAP1-null and WT. These data were confirmed by quantification of mRNA coding for extracellular

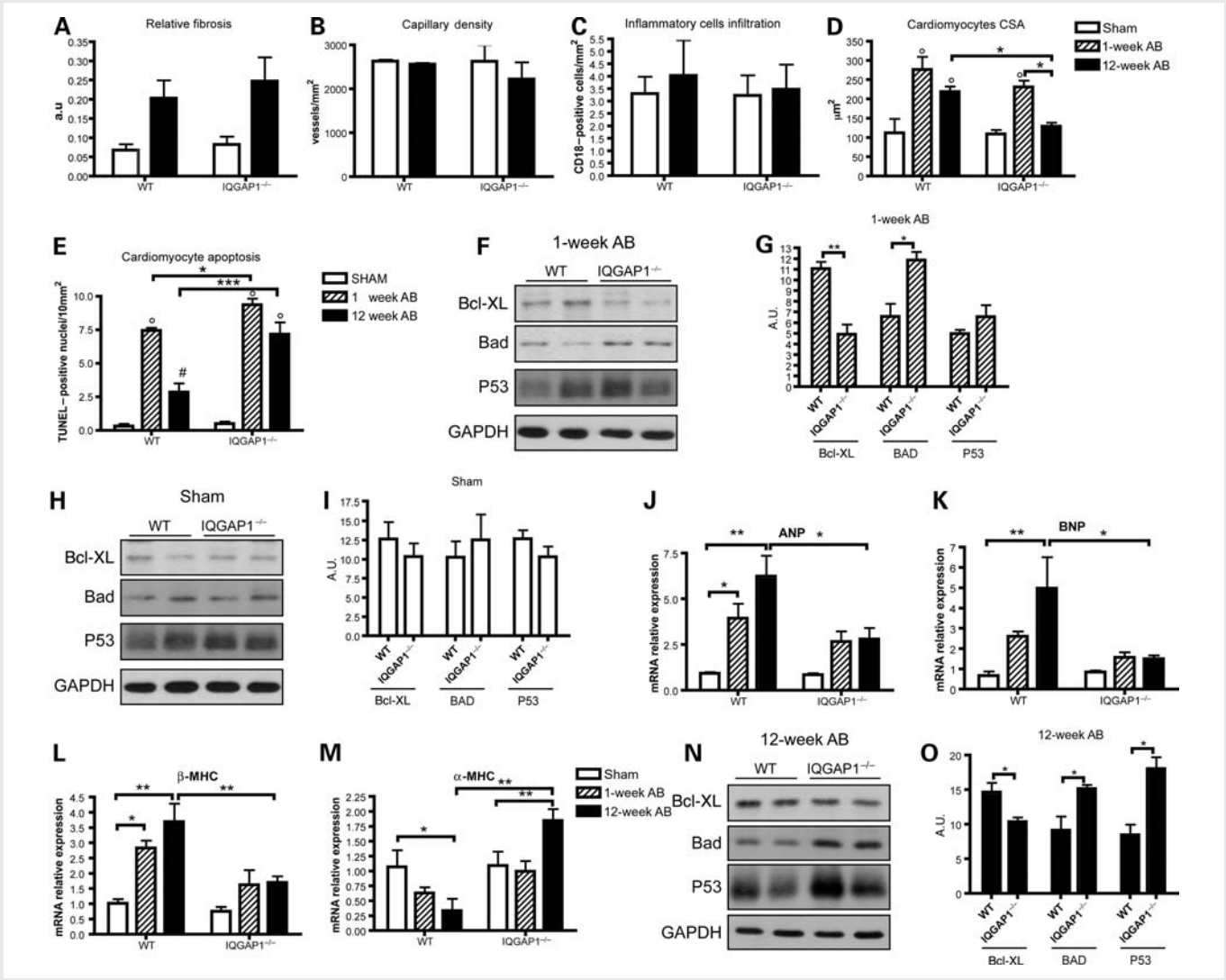


**Figure 3** IQGAP1 is required for cardiomyocyte hypertrophy and survival in response to long-standing pressure overload. Hearts from WT and IQGAP1-null mice (IQGAP1$^{-/-}$), sham-operated or subjected to aortic banding (AB) for 1 or 12 weeks, were analysed. (*A*) Relative fibrosis measured by picrosirius red staining of histological sections ($n = 4$ hearts/group). (*B*) Density of FITC-isolectin-stained capillaries. (*C*) Leucocyte infiltration measured as number of CD18+ cells ($n = 4$ hearts/group). (*D*) Cardiomyocyte cross-sectional area (CSA) ($n = 4$ hearts/group). (*E*) Apoptotic TUNEL-positive cardiomyocytes ($n = 6$ hearts/group for sham and 1-week AB, and $n = 4$ hearts/group at 12-week AB). (*F*) Western blot analysis of Bcl-XL, Bad, and p53 from WT and IQGAP1-null hearts after 1 week of AB; GAPDH was used as a loading control. (*G*) Densitometric quantification of the western blot bands ($n = 4$ hearts/group). (*H*) Western blot analysis of Bcl-XL, Bad, and p53 from sham WT and IQGAP1-null hearts; GAPDH was used as a loading control. (*I*) Densitometric quantification of the western blot bands ($n = 6$ hearts/group). (*J–M*) Real-time PCR of ANP, BNP, β-MHC, and α-MHC mRNAs from sham or 1 and 12 weeks of AB ($n = 6$ hearts/group). (*N*) Western blot analysis of Bcl-XL, Bad, and p53 from WT and IQGAP1-null hearts after 12 weeks of AB; GAPDH was used as a loading control. (*O*) Densitometric quantification of the western blot bands ($n = 6$ hearts/group). $^{\circ}P < 0.05$ vs. sham; $^{*}P < 0.05$; $^{**}P < 0.01$; $^{***}P < 0.001$ $^{\#}P < 0.05$ vs. 1-week AB.

matrix components (collagen I α1, collagen III α1, and fibronectin) (Supplementary material online, *Figure S2A–C*), pro-fibrotic cytokines (TGF-β1 and CTGF) (Supplementary material online, *Figure S2D* and *E*), as well as matrix degrading enzymes, such as metalloproteinase 9 (MMP9) (Supplementary material online, *Figure S2F*). Moreover, the hypoxia-related factor HIF-1α and the pro-angiogenetic cytokine VEGF were unaltered between the two genotypes (Supplementary material online, *Figure S2G* and *H*). Since IQGAP1 is also expressed in fibroblasts, we analysed the possibility that lack of IQGAP1 can alter proliferation and matrix deposition in cardiac fibroblasts, negatively influencing heart remodelling in response to AB. Notably, proliferation and extracellular matrix production and deposition were unaffected in IQGAP1-null neonatal cardiac fibroblasts (Supplementary material online, *Figure S3A–F*).

Interestingly, at 12 weeks of AB, cardiomyocyte hypertrophy was significantly impaired in IQGAP1-null mice compared with WT mice (*Figure 3D*). Moreover, TUNEL analysis clearly demonstrated increased cardiomyocyte apoptosis in IQGAP1-null mice compared with WT (*Figure 3E* and Supplementary material online, *Figure S1C*). Consistent with this finding, western blot analysis on hearts subjected to 12-week AB demonstrated a significantly lower expression of the

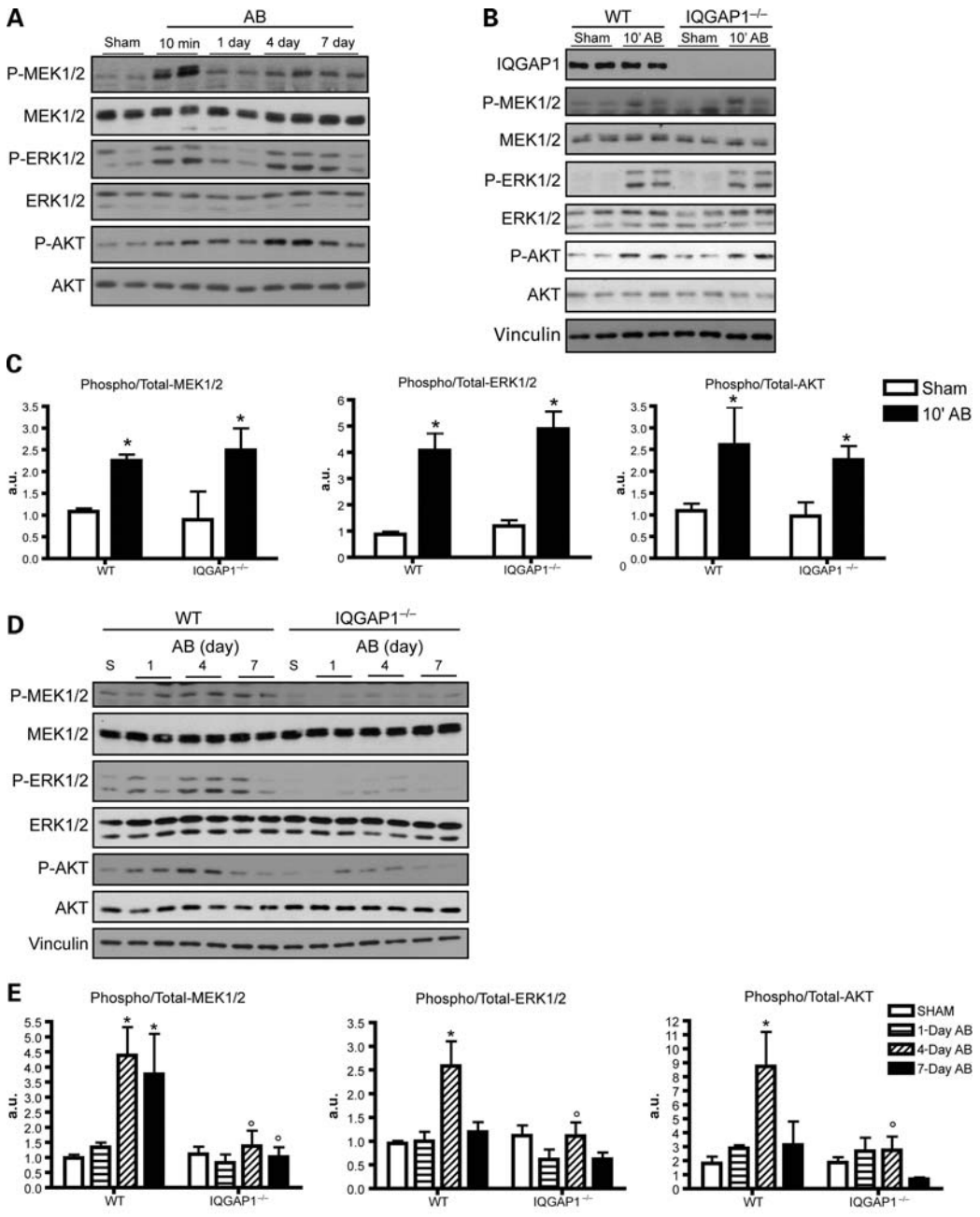


**Figure 4** IQGAP1 mediates the second phase of ERK1/2 and AKT phosphorylation in response to pressure overload. (*A*) Western blot analysis of phosphorylated and total MEK1/2, ERK1/2, and AKT from WT mice subjected to AB for the indicated time. (*B*) Western blot analysis of phosphorylated and total MEK1/2, ERK1/2, and AKT from WT and IQGAP1-null mice subjected to 10 min of AB. (*C*) Quantification of western blot bands, expressed as phospho/total protein ratio ($n = 6$ hearts/group). (*D*) Western blot analysis of phosphorylated and total MEK1/2, ERK1/2, and AKT in WT and IQGAP1$^{-/-}$ hearts subjected to AB for the indicated time. Vinculin was used as a loading control. (*E*) Quantification of western blot bands expressed as phospho/total protein ratio ($n = 4$ hearts/group). *$P < 0.05$ vs. sham; °$P < 0.05$ vs. WT.

pro-survival protein Bcl-XL (*Figure 3N* and *O*). In addition, a higher expression of the pro-apoptotic protein Bad and p53 (*Figure 3N* and *O*) were detected in IQGAP1-null compared with WT mice. Measurements of apoptotic protein transcripts by RT-PCR (not shown) indicated that their altered expression was due to post-transcriptional control.

Expression of both ANP and brain natriuretic peptide (BNP) and β-MHC was strongly upregulated after 12 weeks of AB in WT mice (*Figure 3J–L*). This up-regulation was paralleled by a strong reduction of the α-MHC, consistent with the development of heart hypertrophy induced by AB (*Figure 3M*). However, IQGAP1-null mice failed to upregulate ANP, BNP, and β-MHC (*Figure 3J–L*) and failed to down-regulate α-MHC (*Figure 3M*), thus indicating that IQGAP1 is required for the activation of the foetal gene programme in response to AB.

Overall, these data indicate that in spite of unaltered heart function and organization in basal conditions, upon pressure overload

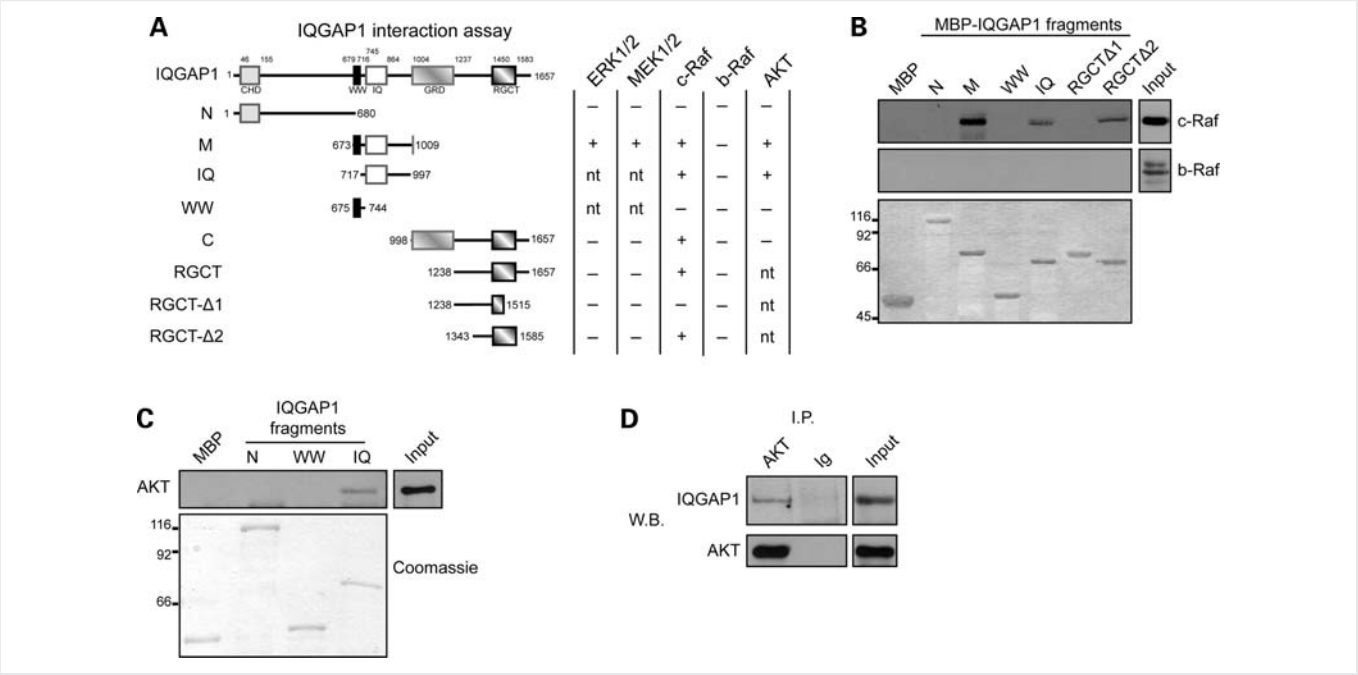


**Figure 5** IQGAP1 interacts with c-Raf, MEK1/2, ERK1/2, and AKT in the heart. (*A*) MBP-fused recombinant IQGAP1 fragments (N, N-terminal fragment; M, middle fragment; C, C-terminal fragment; IQ, IQ domain-containing fragment; WW, WW domain-containing fragment; RGCT, RGCT domain-containing fragment; RGCT-Δ1, RGCT domain-containing fragment deletion mutant 1; RGCT-Δ2, RGCT domain-containing fragment deletion mutant 2). Columns on the right indicate the capability of each fragment to interact (+) or not (−) with the indicated proteins as evaluated by pull-down assays (nt, not tested). (*B* and *C*) Pull-down experiments with MBP-fused IQGAP1 fragments were used to map the c-Raf (*B*) and AKT (*C*) binding region on IQGAP1. This interaction was revealed by western blotting (upper panels). Recombinant proteins used in the pull-down assay were visualized by Coomassie staining (lower panel). (*D*) AKT and IQGAP1co-immunoprecipitation was detected by western blotting. Input: heart total protein extract. Input was analysed in the same blot; however, a lower exposure is shown to allow a precise detection of the reference band. Figures showed representative pull-down and immunoprecipitation analyses that have been performed at least three times with comparable results.

IQGAP1-null mice showed impaired activation of the foetal gene programme, reduced cardiomyocyte hypertrophy, and increased cardiomyocyte apoptosis.

The absence of IQGAP1 impairs the second wave of ERK1/2 and AKT activation in response to pressure overload.

Cardiac tissue remodelling is triggered by intracellular signalling induced by pressure overload. MAPK and AKT are among the best characterized signalling pathways activated by AB and driving cardiomyocyte hypertrophy and survival. Impairment of these signalling pathways has been shown to affect different aspects of cardiac remodelling. Thus, we focused our analysis in the early phase following AB in the attempt to define alterations in signalling events that precede unfavourable remodelling.

First, we investigated the kinetics of ERK1/2 activation and that of its upstream kinase MEK1/2 at different time points following AB in WT mice, and identified two waves of both MEK1/2 and ERK1/2 phosphorylation. The first wave occurred at a very early time point, 10 min after AB, whereas a second wave peaked at 4 days (*Figure 4A*). Similar kinetics were also observed for AKT phosphorylation (*Figure 4A*). As shown in *Figure 4B* and *C*, absence of IQGAP1 did not affect the first wave of MEK1/2-ERK1/2 and AKT activation, but strongly impaired the phosphorylation of MEK1/2-ERK1/2 and AKT after 4 days of AB, indicating that IQGAP1 selectively controls the second wave of AB-induced intracellular signalling (*Figure 4D* and *E*). Notably, the phosphorylation of other stress-activated MAPKs, such as JNK 1/2/3 and p38, was not affected by the absence of IQGAP1 (Supplementary material online, *Figure S4*). Further analysis performed at 12 weeks of AB demonstrated that phosphorylation of MEK1/2-ERK1/2 and AKT was not significantly different from basal levels both in IQGAP1-null and WT mice (Supplementary material online, *Figure S5*).

## 3.3 IQGAP1 binds both c-Raf, MEK1/2, ERK1/2 and AKT in the heart

To investigate possible mechanisms involved in IQGAP1-dependent ERK and AKT activation, we investigated whether IQGAP1 could function as a scaffold molecule for these kinases in the heart.

Using pull-down assays with different IQGAP1 recombinant fragments (*Figure 5A*), we showed that both ERK1/2 and its upstream kinases MEK1/2 bind to the middle region of IQGAP1 (amino acids 673–1009, region M) (*Figure 5A*). We also showed that the middle region of IQGAP1 binds to c-Raf, the kinase responsible for MEK1/2 phosphorylation (*Figure 5A* and *B*). Interestingly, no binding was detected for b-Raf (*Figure 5A* and *B*) despite its presence in the heart and its previous identification as an IQGAP1-interacting protein in epithelial cells.[12]

Since no data are available on c-Raf binding to IQGAP1, we mapped in detail the binding site, using short recombinant fragments. As shown in *Figure 5A* and *B*, binding of c-Raf was restricted to the IQ

fragment (amino acids 717–997, IQ) of the M region. Moreover, a second binding site for c-Raf was detected in the RGCT domain at the C-terminal portion of IQGAP1 (amino acids1515–1585) (*Figure 5A* and *B*).

In addition to c-Raf , MEK1/2, and ERK1/2, we also detected binding of IQGAP1 to AKT from mouse heart protein extracts (*Figure 5A*). To characterize the IQGAP1 domain involved in AKT binding, we performed a pull-down experiment with IQGAP1 deletion mutants and found that AKT binds to the M region of IQGAP1 (M region; amino acids 673–1009) (*Figure 5A*), specifically to the IQ fragment (amino acids 717–997, IQ) of the M region (*Figure 5C*). The interaction of AKT with IQGAP1 was further confirmed by immunoprecipitation of AKT from mouse heart extracts (*Figure 5D*). These data demonstrate the role of IQGAP1 in the heart as a scaffold for both the ERK1/2 cascade and AKT and suggest a crucial role for this molecule in transducing signals, leading to cardiomyocyte survival and hypertrophy maintenance.

# 4. Discussion

IQGAP1 is a ubiquitously expressed multi-domain protein capable of interacting with a number of signalling proteins, including the MAPK family, and controlling different aspects of cell physiology.[13,14] In this work, we disclose, for the first time, a role for IQGAP1 in cardiac signalling and remodelling in response to pressure overload.

*In vivo* gene inactivation indicated that IQGAP1-null mice show no gross defects during development or adult life, but exhibit a number of subtle phenotypes such as gastric hyperplasia,[7] defective neural progenitor cell migration,[15] and defective platelet procoagulant activity under conditions of mechanical shear stress.[16] Our data indicate that IQGAP1-null mice show no alteration in cardiac function in basal conditions. In fact, both LV wall thickness and diameter, as well as contractility, are identical in IQGAP1-null and WT mice. IQGAP1-null mice, however, develop accelerated dilation and contractile dysfunction, compared with WT mice, when subjected to chronic conditions of pressure overload. In fact, upon 12 weeks of AB, IQGAP1-null mice show thinner LV walls, left chamber dilation, and decreased contractility compared with WT mice. Such maladaptive LV remodelling is characterized by cardiomyocyte apoptosis. Apoptotic death is likely to be due to increased Bad and p53 expression and concomitant reduction of Bcl-XL, leading to an unbalanced ratio of pro- and anti-apoptotic signals. A second important defect accounting for unfavourable remodelling in IQGAP1-null mice is reduced cardiomyocyte hypertrophy in mutant mice following 12 weeks of AB. Increased inflammatory infiltrate, fibrosis, capillary rarefaction, and apoptosis are all typical features of maladaptive cardiac remodelling. Interestingly, loss of IQGAP1 selectively impacts on cardiomyocyte apoptosis and hypertrophy in response to long-standing pressure overload without significantly affecting inflammatory infiltrate, stroma deposition, or capillary density. Another possible explanation for this phenotype could reside in the reduction in mechanical force production; further analysis are required to address this possibility.

Our data indicate that IQGAP1-null mice have impaired MEK-ERK1/2 signalling. Their phenotype, indeed, is reminiscent of that reported in mice lacking ERK1/2 or having impaired ERK1/2 phosphorylation.[17] These mice, in fact, have no basal cardiac defects and develop an initial hypertrophic response to AB comparable with that of WT mice. However, these mutant mice show heart decompensation and failure upon chronic stimulus associated with increased cardiomyocyte apoptotic death.[17] Interestingly, however, we found that the absence of IQGAP1 does not affect global MEK-ERK1/2 signalling in the heart, but it selectively impairs a specific signalling wave. We have shown, in fact, that two temporally distinct waves of ERK1/2 and AKT signalling are triggered in the heart in response to pressure overload, consistent with previous findings[18,19]: the first wave occurring as early as 10 min and the second peaking at 4 days following pressure overload. Only the second wave of both MEK1/2-ERK1/2 and AKT signalling is affected in IQGAP1-null mice, whereas the early signal transduction at 10 min after pressure overload is unchanged in these mutant mice.

The selective signalling defect detected in IQGAP1-null mice indicate that the two signalling waves are under the control of distinct molecular mechanisms and highlight the fact that ERK1/2 and AKT activation in response to pressure overload can occur with different patterns of timing and duration.[1] The requirement of IQGAP1 for the second wave of signalling can be explained by the ability of IQGAP1 to bind ERK1/2 as well the upstream kinases MEK1/2 and c-Raf, consistent with the reported scaffold role of IQGAP1 for the MAPK cascade proteins in fibroblasts and epithelial cells.[12,20] We noticed, however, an interesting binding specificity of IQGAP1 towards Raf kinases in the heart. In fact, although Ren *et al.*[12] have shown that b-Raf binds IQGAP1 in fibroblasts and epithelial cells, our data indicate that c-Raf, but not b-Raf, interacts with IQGAP1 in the heart.

The b-Raf gene, through multiple and tissue-specific alternative splicing, encodes several b-Raf isoforms. Since hearts express only some of the described b-Raf isoforms,[21,22] we can speculate that these particular isoforms are not able to bind IQGAP1. Alternatively, cardiac muscle-specific molecules could be required to mediate IQGAP1 binding to c-Raf. Our data demonstrate that IQGAP1, in addition to ERK1/2 cascade components, can also bind AKT in the heart and is needed for its activation in response to pressure overload. This is in agreement with the recent finding that IQGAP1 can function as an AKT scaffold by binding both AKT and mTOR, thus facilitating AKT activation in hepatocellular carcinoma cells.[23,24]

Whereas IQGAP1 is critical for the second signalling wave, other molecular scaffolds are likely to be involved in coordinating the signalling machinery during the first wave of MEK-ERK1/2 and AKT signalling. Such molecules can include KSR, β-arrestin, or other previously described scaffolds.[5,25,26]

The defective AKT and ERK1/2 signalling in IQGAP1-null mice is consistent with increased levels of apoptotic death and impaired maintenance of cardiomyocyte hypertrophy[17,27–29] observed in these mutant mice after AB. Interestingly, an additional feature of IQGAP1-null mice was their impaired ability in activating the transcription of foetal genes, in particular ANP and β-MHC. In fact, after 1 week of AB, ANP and β-MHC are strongly increased in WT mice, but not in IQGAP1 mutants. This alteration was exacerbated at 12 weeks of AB, where IQGAP1-null mice failed to upregulate ANP, BNP, and β-MHC, and consequently failed to downregulate α-MHC. The defective activation of ANP and β-MHC transcription in IQGAP1-null mice can possibly be ascribed to the lack of the second wave of MEK1/2 and ERK1/2 activation. Indeed, it has been reported that the ANP transcription requires ERK1/2 pathway activation.[30–32] The foetal gene programme is known to be reactivated in adult cardiomyocytes in response to pathological stimuli and functions as an adaptive response aimed to protect the stressed heart.[33] In fact, ANP protective effect is clearly demonstrated by the

development of pathological hypertrophy upon pressure overload in mice deficient for ANP receptors in the heart.[34] These findings suggest that the defective upregulation of ANP and BNP can likely contribute to the development of the maladaptive left ventricle remodelling in IQGAP1-null mice after chronic pressure overload. Moreover, increased expression of β-MHC, characterized by low myosin ATPase velocity, favours adaptation to altered workload conditions.[35]

Overall, these data demonstrate for the first time that IQGAP1 is a key molecule in determining adaptive vs. maladaptive cardiac remodelling in response to pressure overload via temporarily restricted AKT and ERK1/2 activation.

# Supplementary material

Supplementary material is available at *Cardiovascular Research* online.

## Acknowledgements

We wish to thank Roberta Ferretti and Radhika Srinivasan for comments on the manuscript. We would also like to thank Daniela Cimino for help in some experiments and Flavio Cristofani and Maddalena Iannicella for assistance and support in animal experiments.

**Conflict of interest:** none declared.

## Funding

This work was supported by grants from EUGeneHeart (LSHM-CT-2005–018833 to G.T.), Regione Piemonte CIPE 2006 to M.B., Regione Piemonte POR F.E.S.R. 2007/2013 'DRUIDI: Piattaforme Innovative per le Scienze della Vita' to G.T. and M.B., Fondazione Veronesi to G.T., and Ricerca corrente e cinquepermille 2010 to G.L.

## References

1. Kehat I, Molkentin JD. Extracellular signal-regulated kinase 1/2 (ERK1/2) signaling in cardiac hypertrophy. *Ann NY Acad Sci* 2010;**1188**:96–102.
2. Claperon A, Therrien M. KSR and CNK: two scaffolds regulating RAS-mediated RAF activation. *Oncogene* 2007;**26**:3143–3158.
3. Good M, Tang G, Singleton J, Remenyi A, Lim WA. The Ste5 scaffold directs mating signaling by catalytically unlocking the Fus3 MAP kinase for activation. *Cell* 2009;**136**:1085–1097.
4. Patel PA, Tilley DG, Rockman HA. Physiologic and cardiac roles of beta-arrestins. *J Mol Cell Cardiol* 2009;**46**:300–308.
5. Brown MD, Sacks DB. Protein scaffolds in MAP kinase signalling. *Cell Signal* 2009;**21**:462–469.
6. Wang S, Watanabe T, Noritake J, Fukata M, Yoshimura T, Itoh N *et al*. IQGAP3, a novel effector of Rac1 and Cdc42, regulates neurite outgrowth. *J Cell Sci* 2007;**120**:567–577.
7. Li S, Wang Q, Chakladar A, Bronson RT, Bernards A. Gastric hyperplasia in mice lacking the putative Cdc42 effector IQGAP1. *Mol Cell Biol* 2000;**20**:697–701.
8. De Acetis M, Notte A, Accornero F, Selvetella G, Brancaccio M, Vecchione C *et al*. Cardiac overexpression of melusin protects from dilated cardiomyopathy due to long-standing pressure overload. *Circ Res* 2005;**96**:1087–1094.
9. Damilano F, Franco I, Perrino C, Schaefer K, Azzolino O, Carnevale D *et al*. Distinct effects of leukocyte and cardiac phosphoinositide 3-kinase {gamma} activity in pressure overload-induced cardiac failure. *Circulation* 2011;**123**:391–399.
10. Sbroggio M, Ferretti R, Percivalle E, Gutkowska M, Zylicz A, Michowski W *et al*. The mammalian CHORD-containing protein melusin is a stress response protein interacting with Hsp90 and Sgt1. *FEBS Lett* 2008;**582**:1788–1794.
11. Patrucco E, Notte A, Barberis L, Selvetella G, Maffei A, Brancaccio M *et al*. PI3K-gamma modulates the cardiac response to chronic pressure overload by distinct kinase-dependent and -independent effects. *Cell* 2004;**118**:375–387.
12. Ren JG, Li Z, Sacks DB. IQGAP1 modulates activation of B-Raf. *Proc Natl Acad Sci USA* 2007;**104**:10465–10469.
13. Brown MD, Sacks DB. IQGAP1 in cellular signaling: bridging the GAP. *Trends Cell Biol* 2006;**16**:242–249.
14. Brandt DT, Grosse R. Get to grips: steering local actin dynamics with IQGAPs. *EMBO Rep* 2007;**8**:1019–1023.
15. Balenci L, Saoudi Y, Grunwald D, Deloulme JC, Bouron A, Bernards A *et al*. IQGAP1 regulates adult neural progenitors in vivo and vascular endothelial growth factor-triggered neural progenitor migration in vitro. *J Neurosci* 2007;**27**:4716–4724.
16. Bahou WF, Scudder L, Rubenstein D, Jesty J. A shear-restricted pathway of platelet procoagulant activity is regulated by IQGAP1. *J Biol Chem* 2004;**279**:22571–22577.
17. Purcell NH, Wilkins BJ, York A, Saba-El-Leil MK, Meloche S, Robbins J *et al*. Genetic inhibition of cardiac ERK1/2 promotes stress-induced apoptosis and heart failure but has no effect on hypertrophy in vivo. *Proc Natl Acad Sci USA* 2007;**104**:14074–14079.
18. Yasukawa H, Hoshijima M, Gu Y, Nakamura T, Pradervand S, Hanada T *et al*. Suppressor of cytokine signaling-3 is a biomechanical stress-inducible gene that suppresses gp130-mediated cardiac myocyte hypertrophy and survival pathways. *J Clin Invest* 2001;**108**:1459–1467.
19. Hoshijima M, Chien KR. Mixed signals in heart failure: cancer rules. *J Clin Invest* 2002;**109**:849–855.
20. Roy M, Li Z, Sacks DB. IQGAP1 is a scaffold for mitogen-activated protein kinase signaling. *Mol Cell Biol* 2005;**25**:7940–7952.
21. Barnier JV, Papin C, Eychene A, Lecoq O, Calothy G. The mouse B-raf gene encodes multiple protein isoforms with tissue-specific expression. *J Biol Chem* 1995;**270**:23381–23389.
22. Hmitou I, Druillennec S, Valluet A, Peyssonnaux C, Eychene A. Differential regulation of B-raf isoforms by phosphorylation and autoinhibitory mechanisms. *Mol Cell Biol* 2007;**27**:31–43.
23. Wang JB, Sonn R, Tekletsadik YK, Samorodnitsky D, Osman MA. IQGAP1 regulates cell proliferation through a novel CDC42-mTOR pathway. *J Cell Sci* 2009;**122**:2024–2033.
24. Chen F, Zhu HH, Zhou LF, Wu SS, Wang J, Chen Z. IQGAP1 is overexpressed in hepatocellular carcinoma and promotes cell proliferation by Akt activation. *Exp Mol Med* 2010;**42**:477–483.
25. Kolch W. Coordinating ERK/MAPK signalling through scaffolds and inhibitors. *Nat Rev Mol Cell Biol* 2005;**6**:827–837.
26. Dhanasekaran DN, Kashef K, Lee CM, Xu H, Reddy EP. Scaffold proteins of MAP-kinase modules. *Oncogene* 2007;**26**:3185–3202.
27. Bueno OF, De Windt LJ, Tymitz KM, Witt SA, Kimball TR, Klevitsky R *et al*. The MEK1-ERK1/2 signaling pathway promotes compensated cardiac hypertrophy in transgenic mice. *EMBO J* 2000;**19**:6341–6350.
28. DeBosch B, Treskov I, Lupu TS, Weinheimer C, Kovacs A, Courtois M *et al*. Akt1 is required for physiological cardiac growth. *Circulation* 2006;**113**:2097–2104.
29. DeBosch B, Sambandam N, Weinheimer C, Courtois M, Muslin AJ. Akt2 regulates cardiac metabolism and cardiomyocyte survival. *J Biol Chem* 2006;**281**:32841–32851.
30. Gusterson R, Brar B, Faulkes D, Giordano A, Chrivia J, Latchman D. The transcriptional co-activators CBP and p300 are activated via phenylephrine through the p42/p44 MAPK cascade. *J Biol Chem* 2002;**277**:2517–2524.
31. Gillespie-Brown J, Fuller SJ, Bogoyevitch MA, Cowley S, Sugden PH. The mitogen-activated protein kinase kinase MEK1 stimulates a pattern of gene expression typical of the hypertrophic phenotype in rat ventricular cardiomyocytes. *J Biol Chem* 1995;**270**:28092–28096.
32. Thorburn J, Frost JA, Thorburn A. Mitogen-activated protein kinases mediate changes in gene expression, but not cytoskeletal organization associated with cardiac muscle cell hypertrophy. *J Cell Biol* 1994;**126**:1565–1572.
33. Rajabi M, Kassiotis C, Razeghi P, Taegtmeyer H. Return to the fetal gene program protects the stressed heart: a strong hypothesis. *Heart Fail Rev* 2007;**12**:331–343.
34. Holtwick R, van Eickels M, Skryabin BV, Baba HA, Bubikat A, Begrow F *et al*. Pressure-independent cardiac hypertrophy in mice with cardiomyocyte-restricted inactivation of the atrial natriuretic peptide receptor guanylyl cyclase-A. *J Clin Invest* 2003;**111**:1399–1407.
35. Lowes BD, Minobe W, Abraham WT, Rizeq MN, Bohlmeyer TJ, Quaife RA *et al*. Changes in gene expression in the intact human heart. Downregulation of alpha-myosin heavy chain in hypertrophied, failing ventricular myocardium. *J Clin Invest* 1997;**100**:2315–2324.